Chem Soc Rev

TUTORIAL REVIEW

Anion encapsulation and dynamics in self-assembled coordination cages†

Cite this: DOI: 10.1039/c3cs60371g

Radu Custelcean

Received 17th October 2013

DOI: 10.1039/c3cs60371g

www.rsc.org/csr

The ability of cationic coordination cages to act as anion receptors is reviewed, with an emphasis on the anion encapsulation chemistry and the dynamics of cage assembly, anion exchange, and other anion-induced structural transformations. The first part of the review describes various examples of anion-encapsulating coordination cages, categorized on the basis of their M_xL_y stoichiometry (M = metal cation; L = organic ligand). The second part deals with the dynamic aspects of anion encapsulation, including the kinetics and mechanism of anion binding, release, and exchange, as well as the structural evolution of the coordination complexes involved.

Key learning points

- Cationic coordination cages have emerged as a promising class of anion receptors, thanks to their ability to encapsulate anions strongly and selectively.
- The encapsulated anions often serve as templates for the cage assembly, leading to binding cavities with good size and shape complementarity for the included anions.
- Internal functionalization of the cage cavities with complementary binding groups can lead to strong and selective anion binding in competitive environments including water.
- Many coordination cages can exchange the encapsulated anion with external anions, apparently *via* a mechanism involving anion ingress and egress through the cage's portals.
- Coordination cages can display complex anion-induced dynamics, including conformational distortions, intercatenations, and architectural rearrangements.

Introduction

Metal-coordination cages self-assembled from chelating high-symmetry polytopic organic ligands (L) and various metal cations (M) have emerged as a distinctive class of supramolecular architectures with interesting host–guest chemistry and high aesthetic appeal. These cages may display different shapes depending on their M_xL_y stoichiometry, the symmetry of the ligand, the coordination geometry of the metal, and the relative spatial orientation of the ligand and metal components. Recent review articles have focused on various aspects of coordination cages, such as structural design principles, self-assembly, and host–guest chemistry.[1–7]

A large fraction of the coordination cages reported to date are positively charged, as they are assembled from neutral ligands and cationic metal centers. As such, they are inherently suitable for encapsulation of anionic guests, and can potentially serve as anion receptors. However, in order for anion recognition to occur, there needs to be an intimate interaction between the cage host and the anion guest, which typically involves a size and shape match between the two partners. Such principles of complementarity have been recognized since the inception of anion coordination chemistry with the report of anion encapsulation by macrobicyclic diamine hosts called katapinands.[8] As clearly articulated early on by Graf and Lehn, anion encapsulation inside rigid molecular cages with cavities internally functionalized with complementary binding groups can lead to exceptional binding strength and selectivity.[9] One drawback associated with classical molecular cage receptors, though, is that their synthesis is typically laborious, involving multi-step reactions and tedious purifications. In this respect, coordination cages have a distinct advantage, as they can often be readily self-assembled from simple ligand and metal components. The relatively strong metal-coordination bonds also ensure that coordination cages are fairly robust, often persisting in highly competitive solvents including water. As a result, coordination cages have recently emerged as a promising class of self-assembled anion receptors.[10,11]

The purpose of this review is to summarize the recent developments on the topic of anion-binding coordination

Chemical Sciences Division, Oak Ridge National Laboratory, Oak Ridge, Tennessee 37831, USA. E-mail: custelceanr@ornl.gov

† Electronic supplementary information (ESI) available. See DOI: 10.1039/c3cs60371g

cages. While some aspects related to this topic have been touched on in recent reviews of broader scope by Ballester[10] and Amouri,[3] this review provides a systematic and focused analysis of anion encapsulation chemistry, with a special emphasis on structural and dynamic aspects of anion recognition and exchange in coordination cages. The focus will be on examples where the anionic guests interact closely with the cage hosts, as opposed to merely serving as charge-balancing counterions. Also, this review will generally not cover those cases where anion encapsulation was solely observed in the crystalline state by X-ray diffraction, with no evidence of anion encapsulation in solution.

Anion encapsulation and exchange in coordination cages

Examples of anion encapsulation have been reported for a variety of coordination cages, which will be categorized in this section based on their M_xL_y stoichiometry. In addition to structural aspects, the discussion will include, where appropriate, the templating role played by the anion in the cage formation, anion exchange in solution, and anion encapsulation selectivity.

M_2L_4 cages

An early example of anion encapsulation in an M_2L_4 coordination cage was reported by McMorran and Steel, who studied PF_6^- encapsulation in $Pd_2(\mathbf{L1})_4^{4+}$ (**1**).[12] The PF_6^- anion bridged the two Pd centers by weak F···Pd coordination bonds (Fig. 1). This cage persisted in DMSO solutions, and ^{19}F NMR showed two separate peaks corresponding to the PF_6^- anions residing inside and outside the cage, indicating slow exchange on the NMR timescale.

A similar approach by Amouri *et al.* led to BF_4^- encapsulation in the $Co_2(\mathbf{L2})_4^{2+}$ cage **2** (Fig. 2).[13] As in the previous example, the anion was weakly coordinated to the two metal centers *via* F···Co interactions. When the cage was crystallized from acetonitrile, a solvent molecule was externally coordinated to each Co center to complete the pseudooctahedral coordination geometry of the metals. However, when a weakly coordinating solvent like nitromethane was used, two external BF_4^- anions were found to coordinate the Co centers instead.[14] The encapsulated tetrafluoroborate anion appears to play a templating role in the cage self-assembly, as in the presence of other anions like NO_3^- or Cl^-, no cage was observed, and different coordination products formed instead. ^{11}B NMR in CD_3CN solutions at room temperature revealed two signals corresponding to the BF_4^- anions inside and outside of the cage, with no evidence of exchange up to 60 °C. This puts a lower limit of 75 kJ mol^{-1} for the free energy of activation for BF_4^- exchange.

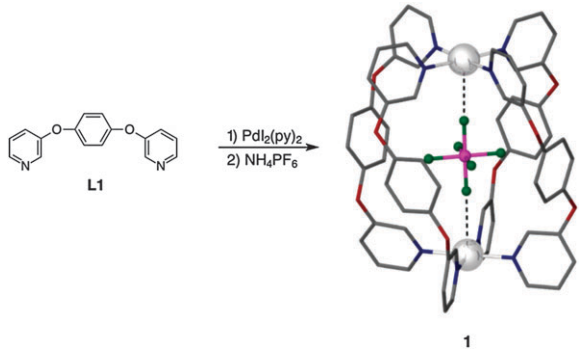

Fig. 1 Encapsulation of PF_6^- in cage **1**. The X-ray crystal structure of the cage is depicted on the right.

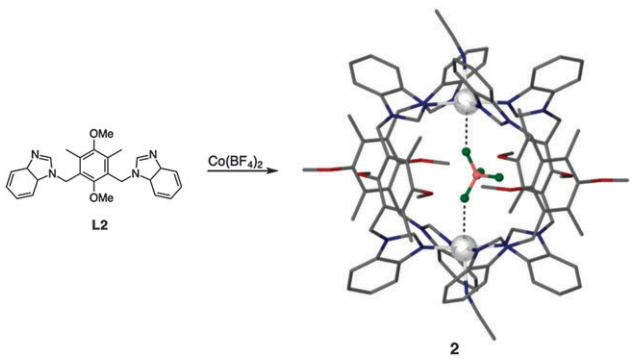

Fig. 2 Encapsulation of BF_4^- in cage **2**. The X-ray crystal structure of the cage is depicted on the right.

M_3L_2 and $M_6L_2L'_3$ trigonal prismatic cages

Reaction of the tripodal tris-benzimidazol ligand **L3** with excess $AgBF_4$ in MeOH/MeCN led to cage **3** with the stoichiometry $Ag_3(\mathbf{L3})_2(BF_4)^{2+}$ (Fig. 3).[15] Single-crystal X-ray crystallography confirmed that one BF_4^- anion was encapsulated inside the cage and it interacted weakly with the silver cations and the benzimidazol CH hydrogens. A similar $Cu_3(\mathbf{L3})_2$ cage encapsulating the CuI_3^- anion was obtained from **L3** and CuI. ^1H NMR spectroscopy indicated the cages formed quantitatively in solution. The anions do not appear to play a templating role,

Radu Custelcean

Radu Custelcean was born in 1972 and grew up in Transylvania, Romania. He studied Chemistry at Michigan State University, where he received his PhD in 2000 for work with James E. Jackson on the structure and reactivity of dihydrogen-bonded crystals. After postdoctoral training in crystal engineering at the University of Minnesota with Michael D. Ward, he started his independent career in 2003 as a research scientist at Oak Ridge National Laboratory. His research interests are in the areas of anion recognition and separation, supramolecular chemistry, and self-assembled molecules and materials for environmental and energy applications.

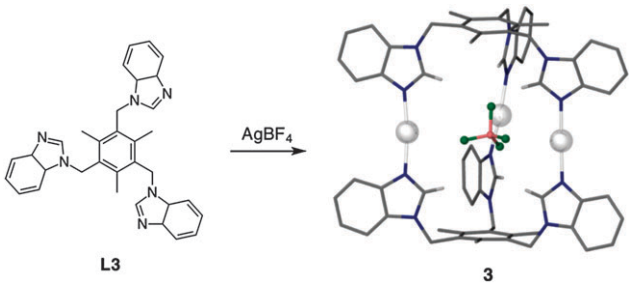

Fig. 3 Encapsulation of BF_4^- in cage **3**. The X-ray crystal structure of the cage is depicted on the right.

as a similar empty cage was obtained when the bulky BPh_4^- anion was used instead.

Reaction of tripodal ligand **L4** with a bis-platinum-1,8-anthracene molecular "clip" yielded the trigonal prismatic cage **4** that was found by X-ray crystallography to encapsulate a nitrate anion (Fig. 4).[16] The NO_3^- anion was tightly bound inside the cavity, as indicated by the fact that it could not be exchanged even in the presence of excess PF_6^-. It was suggested that the observed strong affinity for nitrate in this coordination cage could be a result of the good size and symmetry match between the cage host and the NO_3^- guest.

M_4L_2 cages

Self-assembly of the cavitand ligand **L5** with MX salts (M = Pd, Pt; X = $CF_3SO_3^-$, BF_4^-, PF_6^-) yielded the coordination cages **5** with $M_4(\mathbf{L5})_2^{8+}$ stoichiometry, as determined by NMR and ESI-MS spectroscopies.[17] Single-crystal X-ray diffraction from one of the cages revealed the encapsulation of a highly disordered triflate anion interacting with the resorcinarene rings in the cavity (Fig. 5). Competition experiments in $CDCl_3$, monitored by ^1H and ^{19}F NMR, indicated the following selectivity trend at 300 K: $BF_4^- > CF_3SO_3^- \gg PF_6^-$. The observed selectivity does not correspond to the order expected from the free energy of solvation of the anions in the series. Thus, the smaller BF_4^- anion, which is the most strongly solvated, is preferentially encapsulated. The proposed explanation for the observed selectivity for BF_4^- was that this anion is partly solvated by a molecule of chloroform co-encapsulated in the cage, as evidenced by ESI-MS, and supported by molecular modeling. On the other hand, the other two anions are too big to allow for the inclusion of a solvent molecule. At higher temperatures, though, encapsulation of the larger $CF_3SO_3^-$ was preferred, which was rationalized based on entropic reasons.

M_4L_4 cages

Reaction of the tripodal ligand **L6** with $Eu(ClO_4)_3$ led to the formation of a face-directed tetrahedral $Eu_4(\mathbf{L6})_4^{12-}$ cage (**6**), which was found by X-ray diffraction analysis to encapsulate a perchlorate anion (Fig. 6).[18] The anion does not display any specific interactions, but is held inside the cavity mainly by weak electrostatic interactions. ^{35}Cl NMR analysis revealed two different signals in an approximately 11 : 1 ratio, corresponding to ClO_4^- anions outside and inside the cage that exchange slowly relative to the NMR time scale. Anion exchange experiments found that perchlorate can be exchanged for other

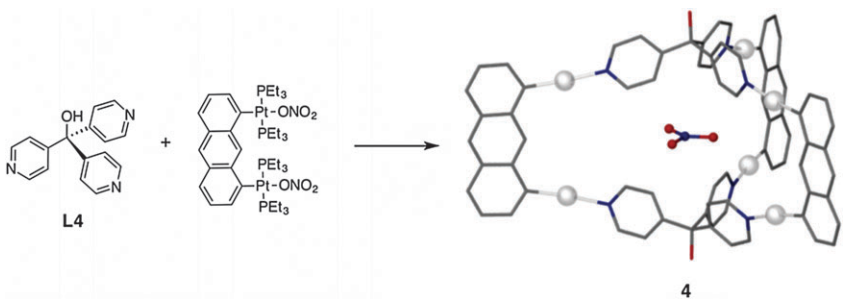

Fig. 4 Encapsulation of NO_3^- in cage **4**. The X-ray crystal structure of the cage is depicted on the right.

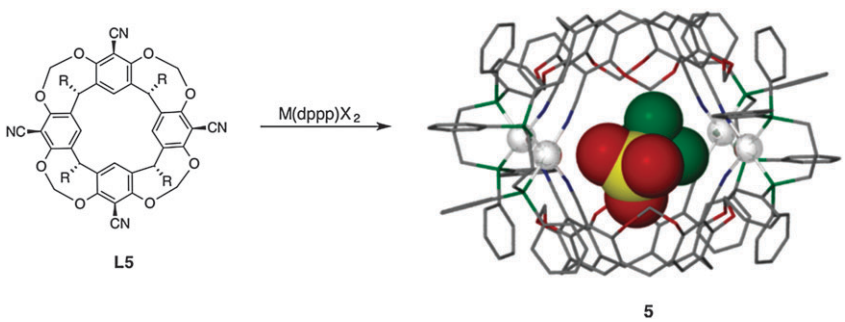

Fig. 5 Encapsulation of $CF_3SO_3^-$ in cage **5**. The X-ray crystal structure of the cage is depicted on the right. M = Pd, Pt; X = $CF_3SO_3^-$, BF_4^-, PF_6^-; dppp = diphenylpropylenephosphene.

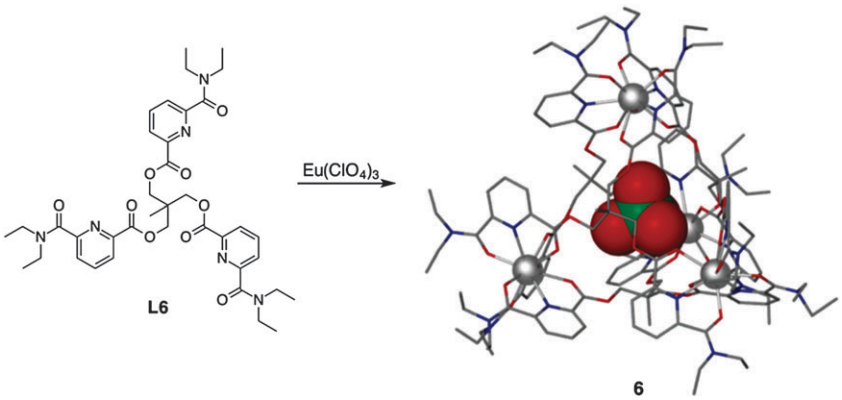

Fig. 6 Encapsulation of ClO_4^- in cage **6**. The X-ray crystal structure of the cage is depicted on the right.

anions such as BF_4^- (K_{ex} = 0.7), imidazolate (K_{ex} = 1.6), or I^- (K_{ex} = 60).

Employment of a larger triptycene-based tripodal ligand led to an analogous $Eu_4L_4^{12-}$ cage that was also found to encapsulate a perchlorate anion. However, in contrast to cage **6**, the encapsulated ClO_4^- was not tightly bound in the larger cavity of this cage, but it rapidly exchanged with perchlorate or other anions like $CF_3SO_3^-$ or BF_4^- outside the cage, as revealed by ^{35}Cl NMR spectroscopy.[19]

M_4L_6 cages

Edge-directed M_4L_6 tetrahedra represent the most common class of anion-encapsulating coordination cages, and were investigated by a number of research groups. An early example was reported in 1996 by Huttner *et al.*, who demonstrated encapsulation of BF_4^- by cage 7 with the $Fe_4(\mathbf{L7})_6^{8+}$ stoichiometry (Fig. 7).[20] The rigidity of the fumaronitrile ligand **L7** was not a prerequisite for the cage formation, as a similar cage could be self-assembled from the more flexible analogous succinonitrile. ^{19}F NMR analysis suggested fast anion exchange at room temperature, as indicated by the presence of a single peak for the BF_4^-. This peak, however, was split into two peaks with a ratio of 1 : 7 at −30 °C, corresponding to encapsulated and free BF_4^- anions, respectively.

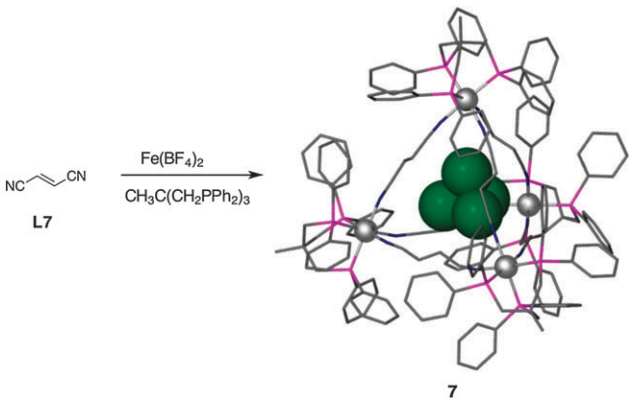

Fig. 7 Encapsulation of BF_4^- in cage **7**. The X-ray crystal structure of the cage is depicted on the right.

exchanged slowly with BF_4^- anions outside the cage, as indicated by ^{11}B and ^{19}F NMR spectroscopy that showed two distinct peaks up to 70 °C.[23] Other tetrahedral anions like ClO_4^- could also template the cage self-assembly, but not the larger and differently shaped PF_6^-, suggesting that size and shape match between the cage host and the anion guest are important for cage formation. Nevertheless, the encapsulation of the octahedrally-shaped SiF_6^{2-} was observed in the analogous cage **9** (Fig. 8b).[24] On the other hand, when the longer ligand **L11** was employed, the resulting cage **10** had an expanded cavity that could accommodate different anions of various sizes and shapes, like BF_4^-, ClO_4^-, PF_6^-, I^-, or NO_3^-.[25,26] Unlike the previously studied cages, whose vertices displayed only *fac* metal coordination geometry, the structure of cage **10** and other analogues consisted of one vertex with *fac*,

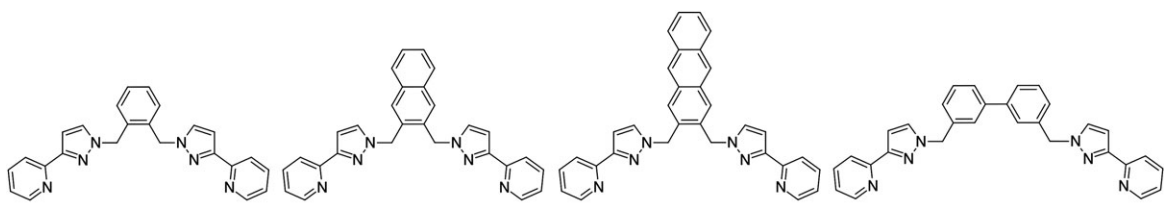

Ward *et al.* reported a number of anion-encapsulating $M_4L_6^{8+}$ cages self-assembled from bis-pyrazolyl-pyridine ligands **L8–11** and various M(II) salts (M = Co, Zn, Cd).[21–26] Their prototype cage $Co_4(\mathbf{L8})_6(BF_4)^{7+}$ (**8**), shown in Fig. 8a, was templated by a BF_4^- anion, which was tightly encapsulated inside the cage cavity *via* C–H···F hydrogen bonds from the methylene groups of the ligands.[21,22] The encapsulated BF_4^-

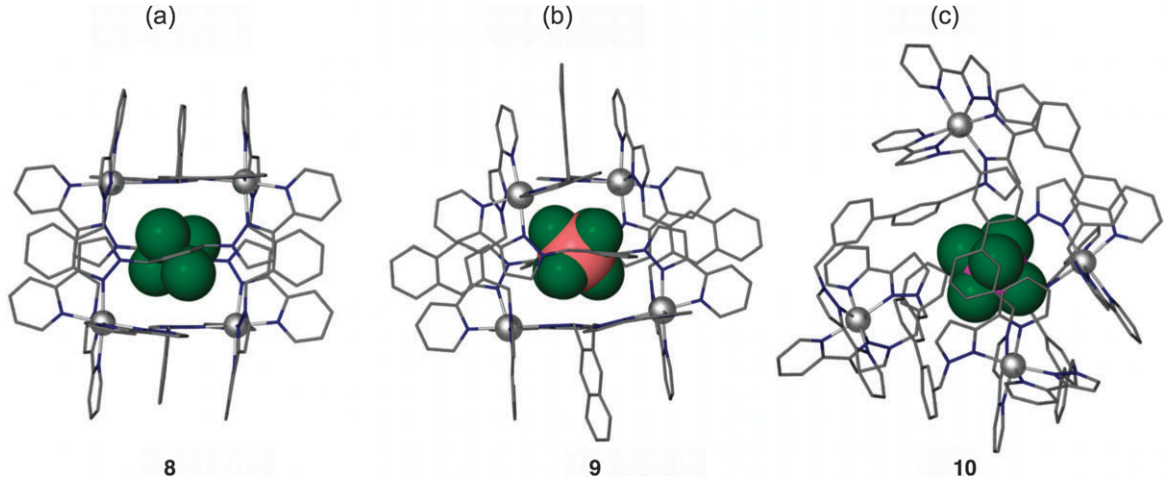

Fig. 8 X-ray crystal structures of M_4L_6 cages **8–10** assembled from **L8**, **L9**, and **L11**, respectively, showing encapsulation of BF_4^- (a), SiF_6^{2-} (b), and PF_6^- (c).

and three vertices with *mer* coordination geometries. No anion templating effect was evident for the assembly of these cages, and the encapsulated anions were found to be displaced from the center of the cavity towards one of the metal vertices, so they can engage in hydrogen bonds with the methylene C–H donors. The encapsulated anions were found at room temperature to undergo fast exchange relative to the NMR time scale. Nevertheless, diffusion NMR spectroscopy (DOSY) experiments at 233 K indicated that BF_4^- anions encapsulated in **10**, as well as in analogous cages assembled from Zn^{2+} or Cd^{2+}, are trapped inside their hosts' cavities and diffuse at the same rate as the cage hosts.[26]

A similar approach using the bis-2,2′-bipyridyl ligand **L12** led to encapsulation of BF_4^- or PF_6^- in $Fe_4(\mathbf{L12})_6^{8+}$ cages (**11**, **12**), as found by single crystal X-ray diffraction (Fig. 9), ESI-MS, and NMR spectroscopy.[27] A cage with no anion included in its cavity was also isolated, suggesting that the anion does not necessarily template the self-assembly of this cage. ^{11}B and ^{19}F NMR spectroscopy indicated fast exchange of the BF_4^- anion, as only one anion peak was observed up to 295 K. On the other hand, the larger PF_6^- anion exchanged slowly on the NMR time scale, up to 350 K. Qualitative anion exchange experiments led to the conclusion that this cage is selective for PF_6^- over BF_4^-.

The $Fe_4(\mathbf{L12})_6^{8+}$ cage was also found to encapsulate the $Fe^{III}Cl_4^-$ anion when its assembly was performed in the presence of $FeCl_2$ in acetonitrile under reflux.[28] The preference for the tetrahedral $FeCl_4^-$ over the PF_6^- anion present in solution suggests a good size and shape match between the cage host and the tetrahedral anionic guest. Furthermore, the preferred encapsulation of $Fe^{III}Cl_4^-$ against $Fe^{II}Cl_4^{2-}$ indicates selectivity for lower-charged, less solvated guests, as previously observed in the encapsulation of cationic guests by anionic cages.[29]

Nitschke *et al.* employed a different approach to cage self-assembly that combined reversible metal coordination and imine condensation reactions. Thus, self-assembly of 3,3′-bipyridine-6,6′-dicarboxaldehyde (**L13**) with aniline and Fe(II) salts led to the tetrahedral cage **13**, which was found to encapsulate various anions such as PF_6^-, $CF_3SO_3^-$, or BF_4^-.[30] However, using the $Fe(NTf_2)_2$ salt (NTf_2 = triflimide) led to the isolation of a cage with no anion included, as found by single crystal X-ray diffraction (Fig. 10). This result suggested that anion templating was not necessary for the cage self-assembly. The stability of the anion-free cage allowed for the measurement of absolute binding constants for BF_4^- ($K_a = 2.3 \times 10^4$), $CF_3SO_3^-$ ($K_a = 5.2 \times 10^4$), and PF_6^- ($K_a = 1.3 \times 10^6$) in acetonitrile. The observed anion selectivity could be rationalized based on the

Fig. 9 Encapsulation of BF_4^- (left) and PF_6^- (right) in $Fe_4(\mathbf{L12})_6^{8+}$ cages **11** and **12**, as determined by X-ray crystallography.

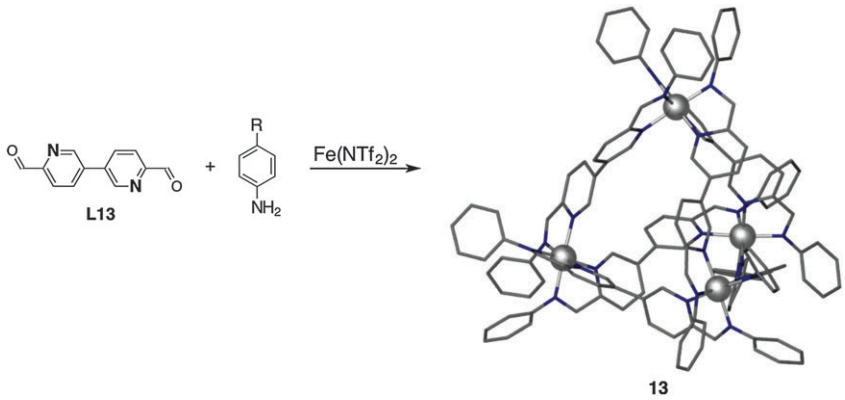

Fig. 10 Self-assembly of cage **13** by reversible metal-coordination and imine condensation. The X-ray crystal structure of the anion-free cage is depicted on the right (the solvent included in the cavity is not shown).

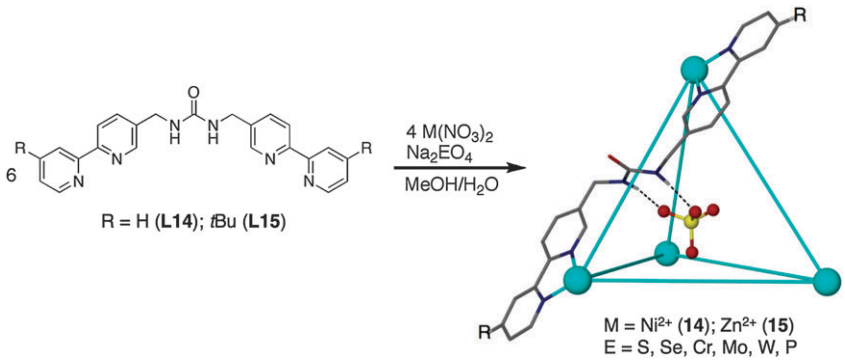

Fig. 11 Self-assembly of urea-functionalized cages **14** and **15** that encapsulate tetrahedral EO_4^{n-} (n = 2, 3) oxoanions. Reproduced with permission from ref. 33. Copyright 2012 American Chemical Society.

anions' packing efficiencies inside the cavity, with the PF_6^- being estimated to occupy an optimal 55% of the cavity.[31]

All coordination cages described to this point have relatively hydrophobic cavities mainly suitable for encapsulating less hydrophilic monocharged anions (*e.g.*, BF_4^-, PF_6^-, ClO_4^-) typically from organic solvents. All these anions have low charge densities that are associated with relatively low free energies of solvation. We had reasoned that effective encapsulation of more hydrophilic, multicharged anions from water requires a new generation of cage receptors functionalized with strong binding groups that can effectively compensate for these anions' high free energy of dehydration. This led to *de novo* design of the M_4L_6 cage receptors **14** and **15** based on the urea-functionalized ligands **L14** and **L15** (Fig. 11), which were found to selectively encapsulate tetrahedral EO_4^{n-} oxoanions (E = S, Se, Cr, Mo, W, P; n = 2, 3) from aqueous solutions.[32,33] Single crystal X-ray diffraction analysis revealed that, as designed, the encapsulated anions accept 12 hydrogen bonds from the 6 chelating urea groups lining the cage cavity (Fig. 12). As a result, the anions are coordinatively saturated and stabilized from the loss of the 12 water molecules from their first hydration shell, resulting in strong binding in aqueous solutions. For example, from competition experiments involving $BaSO_4$ precipitation, the prototypical $Ni_4(\mathbf{L14})_6^{8+}$ cage was found to bind sulfate in water with an apparent association constant greater than 6×10^6 M^{-1}.[32]

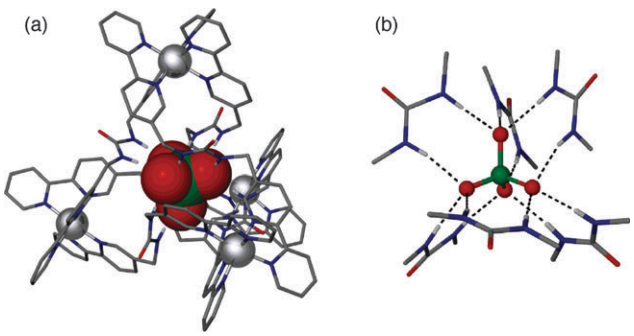

Fig. 12 X-ray crystal structure of PO_4^{3-}@**14** showing the phosphate encapsulation (a) and its binding inside the cavity *via* 12 urea hydrogen bonds (b). Reproduced with permission from ref. 33. Copyright 2012 American Chemical Society.

Further in-depth investigations established that the tetrahedral EO_4^{n-} anions ($n \geq 2$) act as templates for the cage self-assembly. On the other hand, no cage formation was observed with anions of different shapes or charges, including F^-, Cl^-, Br^-, I^-, NO_3^-, BF_4^-, ClO_4^-, ReO_4^-, PF_6^-, AcO^-, $CH_3SO_3^-$, $CF_3SO_3^-$, CO_3^{2-}, SO_3^{2-}, and SeO_3^{2-}. Clearly, the cage self-

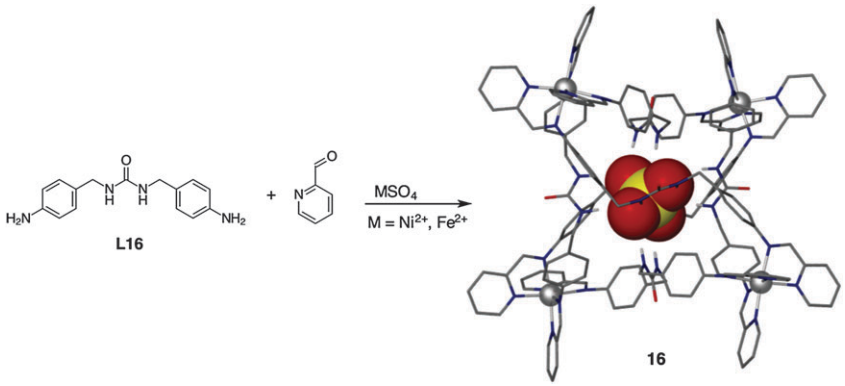

Fig. 13 Self-assembly of urea-functionalized cage **16** by reversible metal-coordination and imine condensation. The X-ray crystal structure of the sulfate-encapsulating cage is depicted on the right.

assembly process is both shape- and charge-selective with respect to the included anion. Quantitative anion exchange experiments with cage **15**, using ^{77}Se NMR spectroscopy and $^{77}SeO_4^{2-}$ as the NMR-active anion, found the following selectivity trend among the EO_4^{n-} anions: $PO_4^{3-} \gg CrO_4^{2-} > SO_4^{2-} > SeO_4^{2-} > MoO_4^{2-} > WO_4^{2-}$. The size of the anions does not appear to play a critical role in determining the observed selectivity due to the relatively high flexibility of the cage, which can distort its structure to accommodate the various sized anions and optimize their hydrogen bonding by the urea groups. More important factors seem to be the anions' charge densities and basicities; as these parameters increase, so do the anions' hydrogen-bond accepting abilities, thereby leading to stronger binding by the urea groups.[33]

Similar urea-functionalized M_4L_6 cage receptors (**16**) were self-assembled from MSO_4 (M = Ni^{2+}, Fe^{2+}) and **L16**, which was condensed *in situ* with 2-formylpyridine to form a bis-iminopyridyl analogue of **L14** (Fig. 13).[34] As in the case of **14** and **15**, the sulfate anion acted as a template for the cage assembly, and no cage formation was observed from other anions such as PF_6^-, ClO_4^-, Cl^-, or PO_4^{3-}. The cage could be disassembled and the sulfate guest released by addition of a strong metal chelator such as tris(2-ethylamino)amine, or by addition of HCl that hydrolyzed the imine bonds and protonated the pyridine groups of the ligand. In the latter case, the process could be reversed by addition of NaOH.

M_6L_8 cages

Reaction of 6 equivalents of amidinothiourea (**L17**) with 8 equivalents of $NiCl_2$ in methanol yielded the $[Ni_6(\mathbf{L17})_8Cl]^{3+}$ coordination cage (**17**), which encapsulated a chloride anion *via* 8 NH···Cl hydrogen bonds and 2 Ni···Cl coordination bonds (Fig. 14).[35] An analogous cage that encapsulated bromide could also be obtained from $NiBr_2$. The halide anions served as templates for the cage formation, and no cage was observed when other anions such as NO_3^-, AcO^-, or ClO_4^- were used instead. Interestingly, the formation of the chloride cage was accompanied by a color change from orange to green, which could be used as the basis for the colorimetric detection of micromolar concentrations of Cl^- in methanol.[36] The cage

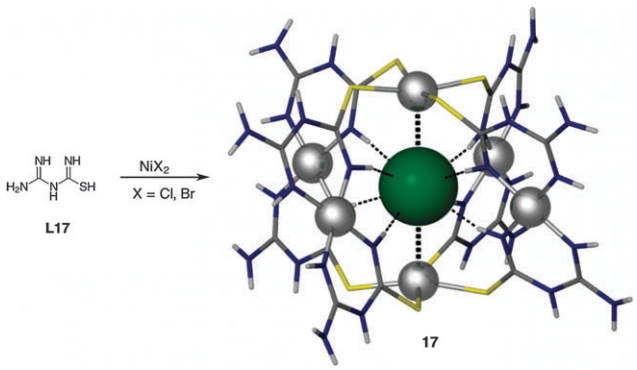

Fig. 14 Encapsulation of Cl^- in cage **17**. The X-ray crystal structure of the cage is depicted on the right.

formation and the color change were exclusively observed with chloride in this solvent. However, in a methanol–acetone mixed solvent, a similar color change was observed with F^- or Br^-, but not with I^-, ClO_4^-, AcO^-, or NO_3^-. Qualitative anion exchange experiments between Cl^- and Br^- indicated the cage preferentially encapsulates the chloride anion.

Dynamics of anion encapsulation

Chemical recognition between the coordination cage hosts and the anionic guests undoubtedly plays a critical role in determining the outcome of the cage assembly (whether a cage forms in the first place), the structure of the resulting cages, and the selectivity of anion encapsulation. Equally important are the dynamics of cage self-assembly and anion encapsulation, specifically the kinetics and mechanism of anion encapsulation, release, and exchange, as well as the structural evolution of the coordination complexes involved. This section will discuss these aspects in various anion-encapsulating coordination cages.

One important question is related to the mechanism of anion encapsulation, release, and exchange in coordination cages. This issue has been recently discussed in the broader context of guest exchange in supramolecular host–guest

assemblies.[37] Generally, there are two possible mechanisms of guest encapsulation and release in metal-coordination assemblies: constrictive, involving expansion of the coordination structures' apertures to allow for guest ingress and egress, or rupture of one or more metal–ligand bonds to create a larger portal for guest exchange. When the whole process of guest exchange is considered, there is also the question whether the guest exchange occurs *via* a concerted, associative (S_N2-like) mechanism, or by a dissociative (S_N1-like) mechanism involving first the guest egress resulting in an empty or solvent-filled cage, followed by uptake of the incoming guest. These issues have been studied in detail for cationic guest exchange in $M_4L_6^{12-}$ coordination cages, which led to the conclusion that, in this class of host–guest systems, a constrictive dissociative mechanism typically operates.[37]

A number of experimental observations provided insight into the mechanism of anion exchange in cationic coordination cages. For example, a lower limit for the free energy of activation for BF_4^- exchange by cage **2** was estimated to be around 75 kJ mol^{-1}.[13] Relatively slow anion exchange was also observed for cage **6**, with measured rates of ClO_4^- exchange by BF_4^- or I^- of 4×10^{-4} and 1.1×10^{-3}, respectively.[18] The fact that the exchange reaction with the smaller I^- is 2–3 times faster is consistent with a constrictive mechanism. A constrictive anion exchange mechanism was also proposed for cage **10**, for which the free energy of activation for BF_4^- and PF_6^- self-exchange was determined to be 50 and 48 kJ mol^{-1}, respectively.[25] The similar activation values observed for these differently sized anions can be rationalized based on the relatively large apertures of **10**, which allow the anions to move in and out with little resistance. It was argued that the alternative mechanism involving partial dissociation of the cage through cleavage of a metal–ligand bond would have required a much larger activation energy.[25]

Molecular dynamics (MD) simulations were employed to gain insight into the mechanism of sulfate exchange in the urea-functionalized cage **14**.[33] Specifically, the question addressed was whether sulfate egress involved partial cage disassembly through dissociation of one or more of the metal–bipyridine coordination bonds, or whether the sulfate could be ejected through one of the face portals through conformational distortion of the cage *via* a constrictive mechanism. Fig. 15 depicts snapshots taken during this simulation showing that the cage is remarkably flexible, severely distorting its structure with the urea groups flipping inside out to assist the sulfate expulsion. No metal–ligand bond dissociation was observed throughout the simulation, suggesting a constrictive mechanism for anion release.

A cage system that dynamically adapts to different anionic guests was studied by Clegg *et al.*[38] Thus, cage **18** with the $Fe_4L_6^{8+}$ stoichiometry was self-assembled from 4,4′-diaminobiphenyl, 2-formylpyridine, and $Fe(NTf_2)$ in acetonitrile (Fig. 16). NMR analysis showed that in solution, **18** is present as a mixture of diastereomers (**18**-*T*, **18**-C_3, **18**-S_4) differing in the relative stereochemistry (Δ or Λ) of the four metal centers. Single crystal X-ray diffraction analysis revealed that the cage crystallized as the S_4 diastereomer and with no anion encapsulated in its cavity. This cage was found to respond to the presence of different anions in solution by changing the ratio of the three diastereomers. For example, the ratio of **18**-*T* : **18**-C_3 : **18**-S_4 changed from 32 : 49 : 19 in the presence of NTf_2^- or triflate (TfO^-), to 64 : 8 : 28, 59 : 26 : 15, and 100 : 0 : 0 in the presence of ClO_4^-, PF_6^-, and BF_4^-, respectively. NMR analysis in solution and X-ray diffraction in the solid state confirmed that the latter three anions were encapsulated inside the cage. An exhaustive thermodynamic analysis led to determination of anion-binding constants for all three diastereomers. Generally, the *T* diastereomer exhibited the strongest binding for most anions, and the highest binding constant of 1.7×10^7 was observed for I^-. The X-ray analysis revealed that the anions are stabilized inside the cage cavity by CH$\cdots$X$^-$ hydrogen bonding, and the cage is highly flexible, adjusting its volume through bond rotations to optimally accommodate the different-sized anions. Thus, this cage system demonstrated extraordinary adaptability in response to external anionic stimuli, responding both at the molecular level through conformational distortions, and at the system level through diastereomeric interconversions. Extensive kinetic measurements also provided

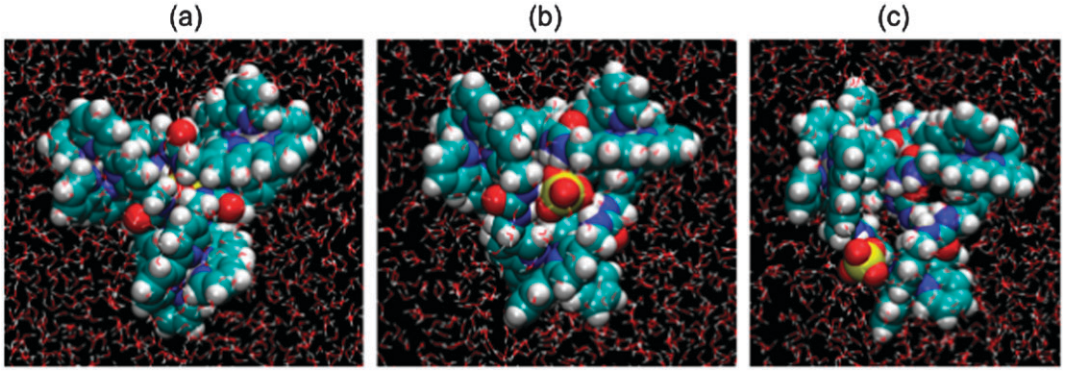

Fig. 15 Snapshots from the MD simulation of sulfate release from **14**: (a) the initial sulfate-encapsulating cage; (b) intermediate structure with the sulfate partly released but still bound to the cage exterior *via* urea hydrogen bonding; (c) final structure with sulfate completely dissociated. A movie of the sulfate release simulation is included in the ESI.†

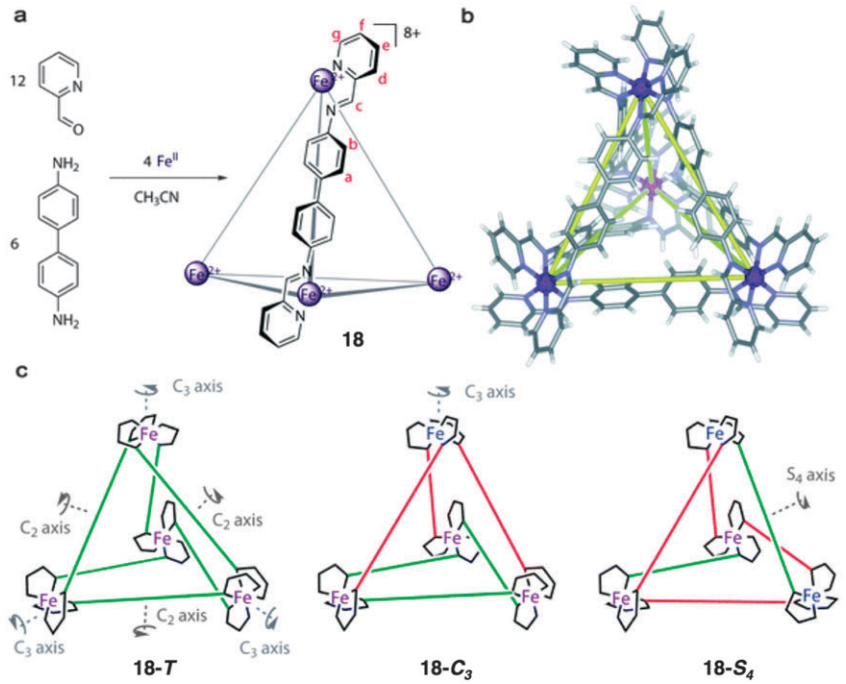

Fig. 16 (a) Self-assembly of cage **18**. (b) X-ray crystal structure of the anion-free **18**. (c) Schematic representation of the three different diastereomers adopted by **18**. Reproduced from ref. 38 with permission from The Royal Society of Chemistry.

mechanistic insight into the cage dynamics, establishing that the relatively slow diastereomer interconversion requires cleavage of the metal–ligand bonds, whereas the much faster anion exchange occurs *via* a constrictive mechanism.

Taking advantage of the different anion affinity of cages **13** and its larger analogue **19**, Nitschke *et al.* devised a more complex system, consisting of a mixture of **13** and **19**, that displayed sequential anion exchange in a chain-reaction fashion (Fig. 17).[39]

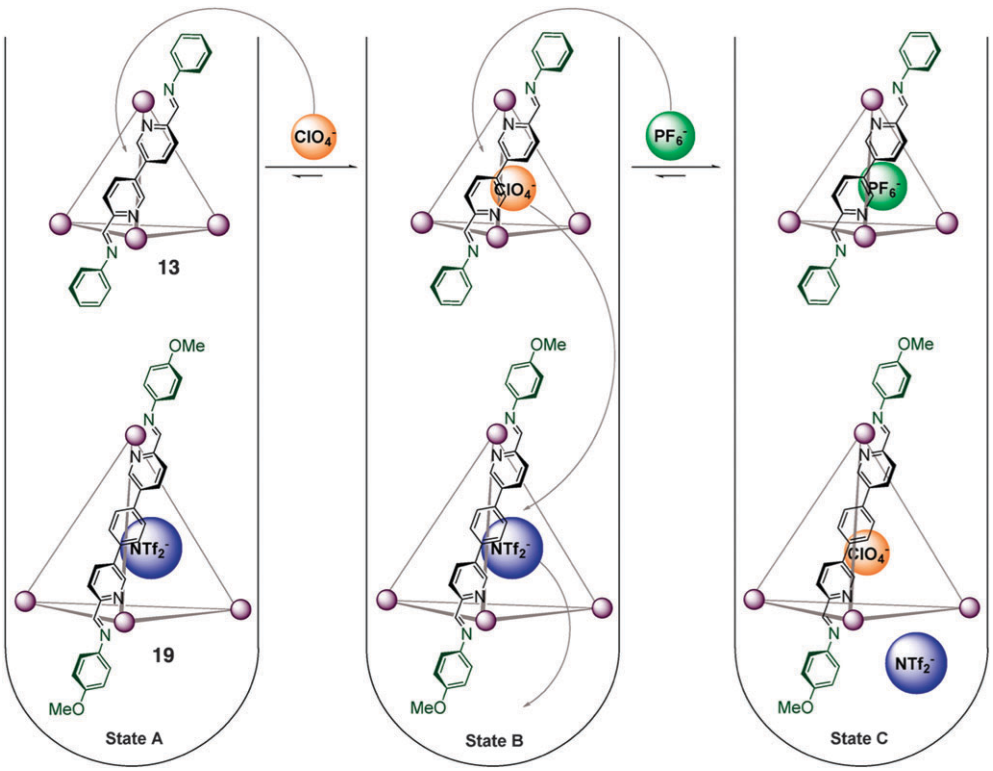

Fig. 17 Sequential anion exchange reactions by cages **13** and **19**. Reproduced with permission from ref. 39. Copyright 2013 American Chemical Society.

In the initial state (state A), cage **19** encapsulated the NTf_2^- anion, which was too large to fit in the cavity of cage **13**. Addition of ClO_4^- led to encapsulation of this anion mainly in **13**, (state B). Finally, addition of PF_6^- led to displacement of ClO_4^- from **13**, which in turn displaced most of the NTf_2^- from **19** (state C). Although the anion selectivity in this chain-reaction exchange was only moderate, demonstration of this concept represents an important first step towards the development of more elaborate chemical systems with anion dynamics approaching the complexity of biological systems.

Nitschke's group also reported another system displaying complex anion-induced dynamics, as depicted in Fig. 18.[40] Self-assembly of 6,6′-diformyl-3,3′-bipyridine with *p*-toluidine and $Co(NTf_2)_2$ yielded a dynamic library consisting of a complex

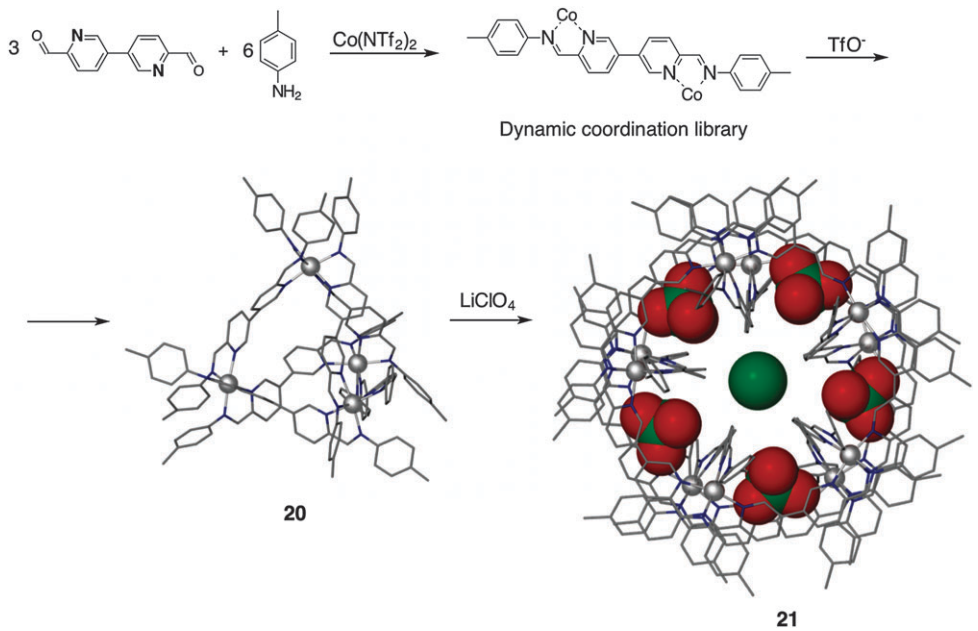

Fig. 18 Anion-controlled self-assembly of tetrahedral cage **20** and barrel-shaped D_5-symmetrical cage **21**.

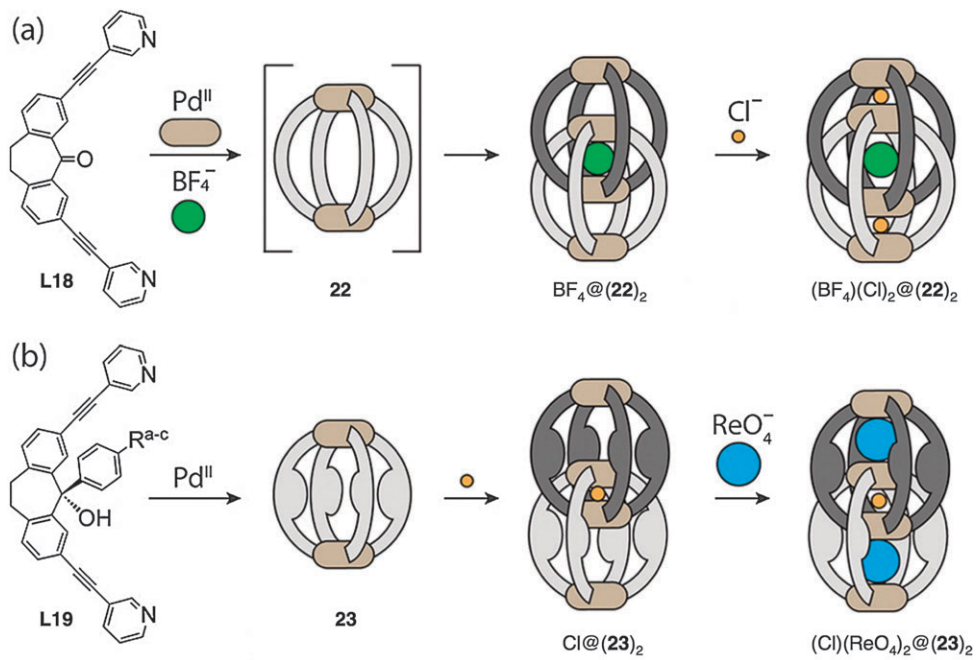

Fig. 19 (a) Self-assembly of cage **22**, and its anion-induced dimerization into the intercatenated cage $(\mathbf{22})_2$ that encapsulated a BF_4^- and two Cl^- anions. (b) Self-assembly of cage **23**, and its anion-induced dimerization into the intercatenated cage $(\mathbf{23})_2$ that encapsulated a Cl^- and two ReO_4^- anions. Reproduced with permission from ref. 43. Copyright 2013 American Chemical Society.

mixture of coordination complexes. Addition of triflate (TfO^-) to this mixture templated the formation of tetrahedral cage **20** as a single product. The same cage could also be templated by the PF_6^- anion. Subsequent addition of $LiClO_4$ induced the structural rearrangement of **20** into the $Co_{10}L_{15}^{20+}$ cage **21**. Single crystal X-ray diffraction analysis of **21** revealed a barrel-shaped D_5-symmetrical cage structure encapsulating $5ClO_4^-$ anions in peripheral binding pockets, and one adventitious Cl^- in the central cavity (Fig. 18). The perchlorate anions templated the cage self-assembly at two different levels. First, they served as templates for the five peripheral binding pockets of the cage, optimally filling their cavities. Second, they templated the formation of the central cavity of the cage, which tightly encapsulated Cl^- by 10CH···Cl hydrogen bonds. This cage displayed very strong binding of chloride, with an estimated association constant greater than 6×10^5 M^-. A similar cage with no anion in the central cavity could also be isolated under more stringent conditions using silver-treated glassware, suggesting that the chloride anion is not needed as a template for the formation of **21**. In addition to ClO_4^-, cage **21** could also be templated by PF_6^-, TfO^-, or mixtures of these two anions.

Clever *et al.* recently reported a unique class of coordination cages with complex anion-encapsulation dynamics.[41–43] Reaction of $[Pd(CH_3CN)](BF_4)_2$ with **L18** initially yielded the $Pd_2(\mathbf{L18})_4^{4+}$ cage **22**, which was thermodynamically unstable and rearranged quantitatively into the dimeric intercatenated cage $(\mathbf{22})_2$ containing a tightly encapsulated BF_4^- in its central cavity, and two loosely bound BF_4^- anions in its outer pockets. The latter could be easily replaced by two halide anions through a positively cooperative anion exchange process in which the binding of the first halide induced a compression of the double cage and facilitated the binding of the second halide (Fig. 19a). Chloride binding in particular was extremely strong, with an estimated net binding constant of 10^{20} M^{-2} that was sufficient to induce dissolution of AgCl in acetonitrile.[41,42]

When the bulkier ligand **L19** was employed, the analogous cage **23** was self-assembled, which was stable as a monomer and did not interpenetrate in the presence of BF_4^- apparently as a result of steric hinderance.[43] Nevertheless, addition of 0.5 equiv. of the smaller Cl^- anion induced cage dimerization through intercatenation, with the chloride now encapsulated in the resulting central cavity (Fig. 19b). Single crystal X-ray diffraction analysis revealed a significantly smaller central binding cavity in the $Cl@(\mathbf{23})_2$ cage compared to $BF_4@(\mathbf{22})_2$ (Fig. 20). This structural compression led in turn to an expansion of the peripheral binding pockets, which as a result became better fitted for encapsulation of larger anionic guests such as ClO_4^-, PF_6^-, or ReO_4^-. The binding of perrhenate was particularly favorable, with measured K_1 and K_2 association constants in acetonitrile of 2158 and 1848 M^{-1}, respectively.[43]

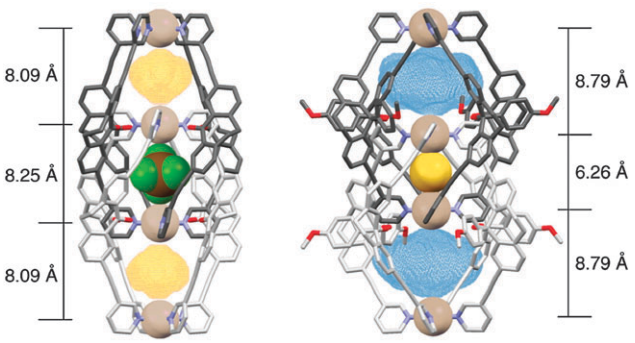

Fig. 20 Crystal structure comparison of $BF_4@(\mathbf{22})_2$ (left) and $Cl@(\mathbf{23})_2$ (right). Reproduced with permission from ref. 43. Copyright 2013 American Chemical Society.

Conclusions

Cationic coordination cages have emerged as a promising class of anion receptors, thanks to their ease of synthesis through self-assembly, and their three-dimensional cavities that can encapsulate anions strongly and selectively. The encapsulated anions often serve as templates for the cage formation, which means the resulting cavities tend to display good size and shape complementarity for the included anions. Many coordination cage receptors can exchange the encapsulated anion with external anions, apparently *via* a constrictive mechanism involving anion ingress and egress through the cage's portals. However, more in-depth mechanistic studies are needed for a complete understanding of this process. For example, many coordination cages are anion-templated and tend to rearrange into other coordination assemblies upon removal of the encapsulated anion. As such, it remains unclear whether the anion exchange occurs through an S_N2-like mechanism, or through a dissociative S_N1-like path that would also involve the rearrangement of the resulting 'empty' coordination cage. Recent studies have shown that coordination cages can display complex dynamics when presented with different anions, including conformational distortions, interpenetrations, and architectural rearrangements.

While most examples of cage receptors reported to date are limited to binding anions with low charge density (*e.g.*, BF_4^-, PF_6^-, ClO_4^-) in relatively nonpolar organic solvents, it was recently demonstrated that internal functionalization of the cage cavities with complementary binding groups can lead to strong and selective anion binding in more competitive environments including water. This approach may soon drive the transition of this class of anion receptors from the realm of basic research into the real world with its complex and demanding problems.

Acknowledgements

This research was sponsored by the Division of Chemical Sciences, Geosciences, and Biosciences, Office of Basic Energy Sciences, U.S. Department of Energy. Dr Xiaohua Zhang is gratefully acknowledged for providing the MD simulation movie of the sulfate release from the urea-functionalized cage **14** (included in the ESI†).

Notes and references

1 N. J. Young and B. P. Hay, *Chem. Commun.*, 2013, **49**, 1354–1379.
2 T. K. Ronson, S. Zarra, S. P. Black and J. R. Nitschke, *Chem. Commun.*, 2013, **49**, 2476–2490.

3 H. Amouri, C. Desmarets and J. Moussa, *Chem. Rev.*, 2012, **112**, 2015–2041.
4 R. Chakrabarty, P. S. Mukherjee and P. J. Stang, *Chem. Rev.*, 2011, **111**, 6810–6918.
5 M. D. Ward, *Chem. Commun.*, 2009, 4487–4499.
6 M. Yoshizawa, J. K. Klosterman and M. Fujita, *Angew. Chem., Int. Ed.*, 2009, **48**, 3418–3438.
7 M. D. Pluth, R. G. Bergman and K. N. Raymond, *Acc. Chem. Res.*, 2009, **42**, 1650–1659.
8 C. H. Park and H. E. Simmons, *J. Am. Chem. Soc.*, 1968, **90**, 2431–2432.
9 E. Graf and J.-M. Lehn, *J. Am. Chem. Soc.*, 1976, **98**, 6403–6405.
10 P. Ballester, *Chem. Soc. Rev.*, 2010, **39**, 3810–3830.
11 R. Custelcean, *Chem. Commun.*, 2013, **49**, 2173–2182.
12 D. A. McMorran and P. J. Steel, *Angew. Chem., Int. Ed.*, 1998, **37**, 3295–3297.
13 H. Amouri, L. Mimassi, M. N. Rager, B. E. Mann, C. Guyard-Duhayon and L. Raehm, *Angew. Chem., Int. Ed.*, 2005, **44**, 4543–4546.
14 H. Amouri, C. Desmarets, A. Bettoschi, M. N. Rager, K. Boubekeur, P. Rabu and M. Drillon, *Chem.–Eur. J.*, 2007, **13**, 5401–5407.
15 C.-Y. Su, Y.-P. Cai, C.-L. Chen, F. Lissner, B.-S. Kang and W. Kaim, *Angew. Chem., Int. Ed.*, 2002, **41**, 3371–3375.
16 C. J. Kuehl, Y. K. Kryschenko, U. Radhakrishnan, S. R. Seidel, S. D. Huang and P. J. Stang, *Proc. Natl. Acad. Sci. U. S. A.*, 2002, **99**, 4932–4936.
17 F. Fochi, P. Jacopozzi, E. Wegelius, K. Rissanen, P. Cozzini, E. Marastoni, E. Fisicaro, P. Manini, R. Fokkens and E. Dalcanale, *J. Am. Chem. Soc.*, 2001, **123**, 7539–7552.
18 B. El Aroussi, L. Guenee, P. Pal and J. Hamacek, *Inorg. Chem.*, 2011, **50**, 8588–8597.
19 J. Hamacek, D. Poggiali, S. Zebret, B. El Aroussi, M. W. Schneider and M. Mastalerz, *Chem. Commun.*, 2012, **48**, 1281–1283.
20 S. Mann, G. Huttner, L. Zsolnai and K. Heinze, *Angew. Chem., Int. Ed. Engl.*, 1996, **35**, 2808–2809.
21 J. S. Fleming, K. L. V. Mann, C.-A. Carraz, E. Psillakis, J. C. Jeffery, J. A. McCleverty and M. D. Ward, *Angew. Chem., Int. Ed.*, 1998, **37**, 1279–1281.
22 R. L. Paul, Z. R. Bell, J. C. Jeffery, J. A. McCleverty and M. D. Ward, *Proc. Natl. Acad. Sci. U. S. A.*, 2002, **99**, 4883–4888.
23 R. L. Paul, Z. R. Bell, J. C. Jeffery, L. P. Harding, J. A. McCleverty and M. D. Ward, *Polyhedron*, 2003, **22**, 781–787.
24 I. S. Tidmarsh, B. F. Taylor, M. J. Hardie, L. Russo, W. Clegg and M. D. Ward, *New J. Chem.*, 2009, **33**, 366–375.
25 R. L. Paul, S. P. Argent, J. C. Jeffery, L. P. Harding, J. M. Lynam and M. D. Ward, *Dalton Trans.*, 2004, 3453–3458.
26 B. R. Hall, L. E. Manck, I. S. Tidmarsh, A. Stephenson, B. F. Taylor, E. J. Blaikie, D. A. V. Griend and M. D. Ward, *Dalton Trans.*, 2011, **40**, 12132–12145.
27 C. R. K. Glasson, G. V. Meehan, J. K. Clegg, L. F. Lindoy, P. Turner, M. B. Duriska and R. Willis, *Chem. Commun.*, 2008, 1190–1192.
28 C. R. K. Glasson, J. K. Clegg, J. C. McMurtrie, G. V. Meehan, L. F. Lindoy, C. A. Motti, B. Moubaraki, K. S. Murray and J. D. Cashion, *Chem. Sci.*, 2011, **2**, 540–543.
29 T. N. Parac, D. L. Caulder and K. N. Raymond, *J. Am. Chem. Soc.*, 1998, **120**, 8003–8004.
30 Y. R. Hristova, M. M. J. Smulders, J. K. Clegg, B. Breiner and J. R. Nitschke, *Chem. Sci.*, 2011, **2**, 638–641.
31 S. Mecozzi and J. Rebek Jr., *Chem.–Eur. J.*, 1998, **4**, 1016–1022.
32 R. Custelcean, J. Bosano, P. V. Bonnesen, V. Kertesz and B. P. Hay, *Angew. Chem., Int. Ed.*, 2009, **48**, 4025–4029.
33 R. Custelcean, P. V. Bonnesen, N. C. Duncan, X. Zhang, L. A. Watson, G. Van Berkel, W. B. Parson and B. P. Hay, *J. Am. Chem. Soc.*, 2012, **134**, 8525–8534.
34 S. Yi, V. Brega, B. Captain and A. E. Kaifer, *Chem. Commun.*, 2012, **48**, 10295–10297.
35 R. Vilar, D. M. P. Mingos, A. J. P. White and D. Williams, *Angew. Chem., Int. Ed.*, 1998, **37**, 1258–1261.
36 P. Diaz, D. M. P. Mingos, R. Vilar, A. J. P. White and D. J. Williams, *Inorg. Chem.*, 2004, **43**, 7597–7604.
37 M. D. Pluth and K. N. Raymond, *Chem. Soc. Rev.*, 2007, **36**, 161–171.
38 J. K. Clegg, J. Cremers, A. J. Hogben, B. Breiner, M. M. J. Smulders, J. D. Thoburn and J. R. Nitschke, *Chem. Sci.*, 2013, **4**, 68–76.
39 S. Ma, M. M. J. Smulders, Y. R. Hristova, J. K. Clegg, T. K. Ronson, S. Zarra and J. R. Nitschke, *J. Am. Chem. Soc.*, 2013, **135**, 5678–5684.
40 I. A. Riddell, M. M. J. Smulders, J. K. Clegg, Y. R. Hristova, B. Breiner, J. D. Thoburn and J. R. Nitschke, *Nat. Chem.*, 2012, **4**, 751–756.
41 S. Freye, J. Hey, A. Torras-Galan, D. Stalke, R. Herbst-Irmer, M. John and G. H. Clever, *Angew. Chem., Int. Ed.*, 2012, **51**, 2191–2194.
42 S. Freye, D. M. Engelhard, M. John and G. H. Clever, *Chem.–Eur. J.*, 2013, **19**, 2114–2121.
43 S. Freye, R. Michel, D. Stalke, M. Pawliczek, H. Frauendorf and G. H. Clever, *J. Am. Chem. Soc.*, 2013, **135**, 8476–8479.

